EURASIP Journal on
Wireless Communications and Networking
a SpringerOpen Journal

RESEARCH   **Open Access**

Capacity-maximization threshold design for wideband sensing with guaranteed minimum primary user rate

Peng Jia and Tho Le-Ngoc[*]

Abstract

We investigate the design of optimal threshold for energy detection of primary user (PU) beacon signals in spectrum sensing. The weighted sum of the PU and secondary user (SU) link rates is used as the objective function with constraint on the guaranteed minimum PU link rate. SU with wideband sensing capability selects the idle frequency-slot with the lowest sensed power to be the candidate to access. Numerical results show that the wideband sensing capability with the proposed optimal threshold and accessing strategy can help the SU to meet the stringent PU rate constraints while achieving much higher SU link rate and network capacity.

Keywords: Cognitive radio, Spectrum sensing, Capacity, Wideband sensing

1. Introduction

Cognitive radio (CR) [1] is promising to leverage the spectrum holes which hide in the grossly underutilized licensed band due to the inflexible spectrum management [2,3]. To achieve this, the secondary user (SU) must be aware of their surrounding environments. Usually, SU performs spectrum sensing to obtain information of the licensed band usage. In this process, different techniques can be used while the simplest one is energy detection which requires no pre-knowledge of the primary user (PU) signal. However, one of the biggest challenges in energy detection is how to design the sensing threshold. Our earlier work [4] investigated the performance of different optimal sensing thresholds derived according to both classic Bayesian and capacity-maximization sensing objectives, indicating that in the communication systems, optimizing *miss detection* and *false alarm* probabilities is just the intermediate step while the network capacity should be optimized. Bayesian method is found to be more PU link rate protective while unconstrained maximization of network capacity may jeopardize the PU link rate to a much higher degree.

To maintain the performance of PU link, in this article,[a] we include the constraint on the guaranteed minimum PU

rate in capacity-maximization threshold design for cognitive sensing. Furthermore, we consider SU with wideband sensing capability and PU transmission of imbedded pilot signals, so that SU can sense PU activity in a number of frequency slots of the licensed PU frequency band and select the suitable idle frequency slot for SU transmission. In this way, the SU may have more than *one* choice, and an appropriate selection algorithm can help to enhance the sensing reliability, which can in turn protect better the PU link rate while improving the achievable SU rate and sum capacity. From the viewpoint of reducing miss detection, we propose the SU to select the frequency slot with the lowest sensed power to be the candidate to access. Based on this wideband sensing approach, we further formulate the network capacity optimization problem with the guaranteed PU link rate, and derive the corresponding optimum threshold. The merits of the wide-band sensing and the corresponding access algorithm are firmly supported by the simulation results as compared to the narrow-band sensing case.

The remainder of this article is organized as follows: Section 2 introduces the single PU and single SU spatial network model and the wideband sensing channel model which includes both large- and small-scale fadings. Furthermore, the network capacity under the wideband operation is derived in Section 3. Section 4 defines the sensing objective function and the constraint function,

* Correspondence: tho.le-ngoc@mcgill.ca
Department of Electrical and Computer Engineering, McGill University,
Montreal, QC H3A 0E9, Canada

Springer

and we also derive the optimal sensing threshold in this section as well. In Section 5, numerical results are illustrated to show the benefits of the wideband sensing and the spectrum access algorithm. Finally, Section 6 concludes this article.

2. Network and channel model

2.1. Network model

Figure 1 illustrates the network model under consideration. The SU transmitter (ST) location is used as the reference point, i.e., the origin of the polar coordinates (0, 0). The SU receiver (SR) is assumed to be uniformly located in a circular area centered at the ST with radius D_S where $d_s \leq D_S$ denotes the distance between ST and SR. ST can introduce noticeable interference to the PU receiver (PR) if the ST–PR distance, d_{SP}, is within the impact distance D_I. The PU transmitter (PT) lies in a circular area centered at the PR with radius D_P and $d_p \leq D_P$ denotes the PT–PR distance. d_{PS*} is the distance between the PT and ST. We also assume a minimum allowable transmitter–receiver distance of ε.

2.2. Sensing channel model

Consider a segment of the licensed PU operation frequency band of B Hz. This segment can have contiguous or non-contiguous spectra with a total bandwidth of W Hz (where $W < B$), which can be divided into K equal frequency slots. PU transmission in each frequency slot of $\Delta f = W/K$ Hz is assumed to be a statistically independent event with *a priori* probability (or PU transmission activity factor) λ. The channel between any *Tx–Rx* pair of distance d over the wide frequency band of B Hz, including large-scale path loss and small-scale multipath

Figure 1 Network model.

fading, can be represented by the following channel impulse response

$$h(t) = h_0 d^{-\alpha/2} \sum_{l=0}^{L-1} h_{Fl}\delta(t - l\Delta t)$$
$$= \sum_{l=0}^{L-1} h_l\delta(t - l\Delta t) \qquad (1)$$

where $\Delta t = 1/B$, $h_l = h_0 d^{-\frac{\alpha}{2}} \cdot h_{Fl}$, d is the distance between the transmitter and receiver, α is the path loss exponent, L is the number of resolvable paths and the tap coefficient of the lth resolvable path, h_{Fl}, is assumed to be a complex circular Gaussian random variable having statistically independent real and imaginary components with zero mean and variance $\sigma_l^2 = \frac{e^{-l/L}}{\sum_{l=0}^{L-1} e^{-l/L}}$.

2.3. Sensing structure

In each frequency slot, PU sends a beacon (e.g., a sinewave tone or a preamble known by SU), which can be regarded as deterministic signal, to assist SU to detect the spectrum occupation (e.g., [5]). We consider the SU having wideband sensing capability so that it can sense the PU beacon signals in a number of frequency slots to select *one* vacant slot for transmission as follows. To resolve the wideband channel into a number of narrowband frequency slots, the SU uses the sensing structure as shown in Figure 2. The wideband sample is first taken as input of the N-point Fast Fourier transform (FFT) to obtain the sensed beacon signals in K subcarriers of the interested frequency segment (where $K < N$ and $\Delta f = B/N$). The power values, ρ_k' s, of the sensed subcarrier beacons are then measured using energy detection and the minimum value, i.e., $\rho_j = \min_{k=1,2,...,K}\rho_k$ is selected for further comparison with the optimal threshold to finally decide on the status (i.e., vacant or occupied) of frequency slot j.

In the frequency domain, via discrete Fourier transform, the discrete frequency response in kth frequency slot is

$$H_k = \sum_{l=0}^{L-1} h_l e^{-j2\pi(l\Delta t)(k\Delta f)} = \sum_{l=0}^{L-1} h_l e^{-\frac{j2\pi lk}{N}} \qquad (2)$$

From the characteristics of h_l's, it can be shown that

$$H_k \sim CN\left(0, h_0^2 d^{-\alpha}\right) \qquad (3)$$

Then, for each frequency slot, the ST needs to perform a binary hypothesis testing to decide between the following two hypotheses:

$$\mathcal{H}_{0,k} : Y_k = V_k \qquad (4)$$

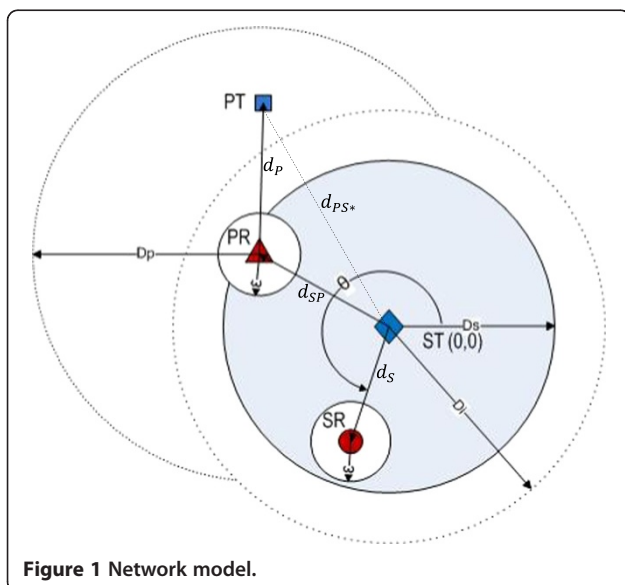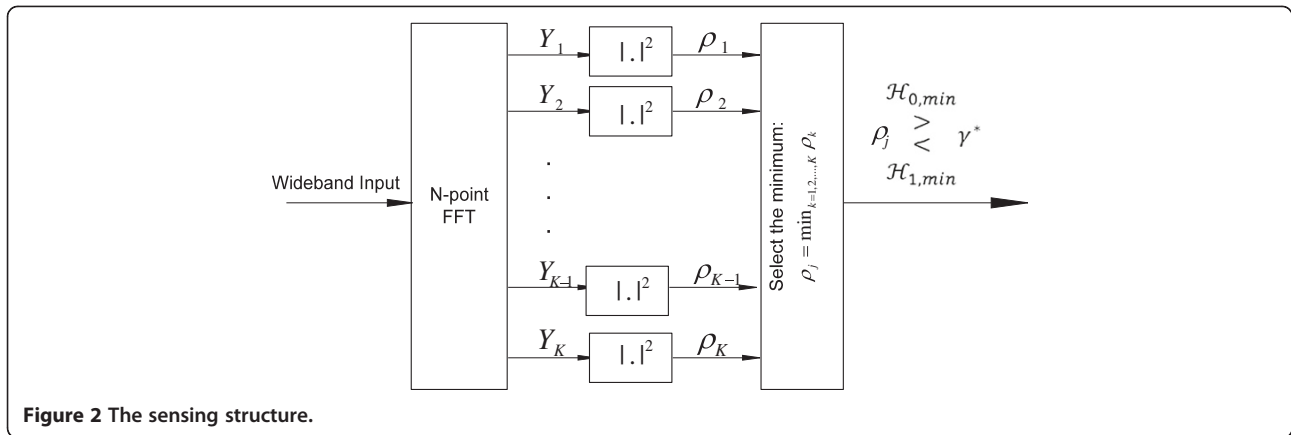$$\mathcal{H}_{1,k} : Y_k = H_k X_k + V_k \qquad (5)$$

Figure 2 The sensing structure.

where $\mathcal{H}_{0,k}$ and $\mathcal{H}_{1,k}$ denote the absence and presence of PU transmission in the kth frequency slot, respectively. X_k is the beacon signal transmitted by PU with power S_{PB} and $V_k \sim CN(0, \sigma_0^2)$ is the complex Gaussian thermal noise in the kth frequency slot. It follows that the sensed power sample in the kth frequency slot, $|Y_k|^2$, is exponentially distributed with the probability density function

$$f_k(y) = r_k e^{-r_k y}, \tag{6}$$

where $r_k = \left\{ \begin{array}{l} 1/\sigma_0^2 \ for \ \mathcal{H}_{0,k} \\ 1/\left(\sigma_X^2 + \sigma_0^2\right) \ for \ \mathcal{H}_{1,k} \end{array}, \sigma_X^2 = S_{PB} h_0^2 d_{PS_*}^{-\alpha}, \right\}$ and recall that d_{PS_*} is the distance between the PT and ST.

3. Network and capacity formulation

Consider the PU transmission in K frequency slots with equal probability λ and equal power S_P. The SU keeps sensing every frequency slot and chooses the minimum sampled power to compare with the optimal threshold. If the sampled power is smaller than the predefined threshold, then the SU will perceive the corresponding frequency slot which is idle and initiate its communication. However, in this cognitive process, the SU will not be able to perfectly detect the idle/occupied frequency slot. Since *miss detection* will bring interference to the PU and *false alarm* will waste SU's precious transmission opportunities, they will both have the impact on the network capacity. For a threshold γ used in the selected frequency slot, the *conditional* probabilities of miss detection $P_m(\gamma)$ and false alarm $P_f(\gamma)$ can be derived as

$$P_m(\gamma) = \int_0^\gamma \frac{e^{-\frac{\xi}{\sigma_0^2 + \sigma_X^2}}}{\sigma_0^2 + \sigma_X^2} d\xi = 1 - e^{\frac{-\gamma}{\sigma_0^2 + \sigma_X^2}}, \tag{7}$$

and

$$P_f(\gamma) = \int_\gamma^\infty \frac{e^{-\frac{\xi}{\sigma_0^2}}}{\sigma_0^2} d\xi = e^{-\frac{\gamma}{\sigma_0^2}}. \tag{8}$$

For the sensing structure and spectrum accessing strategy shown in Figure 2, and independently and exponentially distributed $|Y_k|^2, k = 1, 2, \ldots, K$, the probability that the minimum power sample is in the frequency slot $k*$ can be derived as $P\left(|Y_{k_*}|^2 \leq \forall |Y_k|^2\right) = \int_0^\infty r_{k*} e^{-\sum_{k=1}^K r_k y} dy = \frac{r_{k*}}{\sum_{j=1}^K r_j}$.

In a given time, the PU may occupy q frequency slots, where $0 \leq q \leq K$ with the probability of $P_q = \lambda^q (1 - \lambda)^{(K-q)}$. In the q occupied frequency slots, $r_j = (\sigma_0^2 + \sigma_X^2)^{-1}$, while in the $(K - q)$ vacant frequency slots, $r_k = \sigma_0^{-2}$. Therefore, $\sum_{j=1}^K r_j = \frac{q}{(\sigma_0^2 + \sigma_X^2)} + \frac{(K - q)}{\sigma_0^2}$. It follows that, for a given situation with q occupied frequency slots and $(K - q)$ *vacant* frequency slots, the *conditional* probability that the minimum power sample is in an *occupied* frequency slot is $P_{oq} = \left(\sigma_0^2 + \sigma_X^2\right)^{-1} \left[\frac{q}{(\sigma_0^2 + \sigma_X^2)} + \frac{(K-q)}{\sigma_0^2}\right]^{-1}$, and the *conditional* probability that the minimum power sample is in a *vacant* frequency slot is $P_{vq} = \sigma_0^{-2} \left[\frac{q}{(\sigma_0^2 + \sigma_X^2)} + \frac{(K-q)}{\sigma_0^2}\right]^{-1}$. Subsequently, the probability that the minimum power sample is in the area of *occupied* frequency slots can be expressed as

$$P_o = \sum_{q=0}^K \binom{K}{q} P_q q P_{oq} \tag{9}$$

$$= \sum_{q=0}^K \binom{K}{q} \frac{\lambda^q (1 - \lambda)^{(K-q)} q}{q + (K - q)(1 + \sigma_X^2/\sigma_0^2)}.$$

Similarly, the probability that the minimum power sample is in the area of *vacant* frequency slots can be expressed as

$$P_v = \sum_{q=0}^{K} \binom{K}{q} P_q(K-q) P_{vq}$$

$$= \sum_{q=0}^{K} \binom{K}{q} \frac{\lambda^q (1-\lambda)^{(K-q)}(K-q)\left(1+\sigma_X^2/\sigma_0^2\right)}{q+(K-q)(1+\sigma_X^2/\sigma_0^2)}. \tag{10}$$

It is interesting to verify that $P_o + P_v = 1$, and for $K = 1$, $P_o = \lambda$, $P_v = 1 - \lambda$.

When miss detection occurs, the SU transmits and hence introduces interference to the PU in only *one* *occupied* frequency slot with the probability of $P_m(\gamma) P_o/K$. In this event, the PU rate in the presence of SU interference is $\log_2\left[1+\frac{L_{PK}}{I_S+\sigma_0^2}\right]$ (in b/s/Hz) where $L_{PK} = S_{PK}\left|\frac{1}{\sqrt{N}}\sum_{l=0}^{L-1} h_{FPl} e^{-\frac{j2\pi lk*}{N}}\right|^2$ is the PU signal power received at the PR with $S_{PK} = KS_P$, $h_{FPl} = h_0 \cdot d_P^{-\frac{\alpha}{2}} h_{Fl}$, $I_S = S_S h_0^2 d_{SP}^{-\alpha}|h_{FSP}|^2$ represents the interference from SU to PR, and σ_0^2 is the thermal noise power in a certain frequency slot. Otherwise, in the absence of SU interference, with the probability of $[\lambda - P_m(\gamma) P_o/K]$, the PU rate in the presence of SU interference is $\log_2\left[1+\frac{L_{PK}}{\sigma_0^2}\right]$ (in b/s/Hz). In other words, the PU link rate of a certain frequency slot can be represented as

$$C_{PU} = E\left\{\left(\lambda - \frac{P_m(\gamma) P_o}{K}\right)\log_2\left[1+\frac{L_{PK}}{\sigma_0^2}\right]\right.$$

$$\left. + \frac{P_m(\gamma) P_o}{K}\log_2\left[1+\frac{L_{PK}}{I_S+\sigma_0^2}\right]\right\}\text{(in b/s/Hz),} \tag{11}$$

where $E\{.\}$ represents the expectation over fading and all PU and SU radio locations in the network.

When the false alarm occurs, SU will not transmit (while the frequency slot is actually vacant), effectively introducing capacity loss. This event occurs with the probability of $P_f(\gamma) P_v$. In other words, the event that frequency slot is actually vacant and the SU correctly detects the absence of the PU with the probability of $[1 - P_f(\gamma)]P_v$, and, in this case, the SU can transmit in the vacant frequency slot with the rate of $\log_2\left[1+\frac{L_S}{\sigma_0^2}\right]$ (in b/s/Hz) where $L_S = S_S h_0^2 d_S^{-\alpha}|h_{FS}|^2$ is the SU signal power received at the SR. On the other hand, in the event of miss detection, SU transmits in an *occupied* frequency slot in the presence of interference from the PU with the probability of $P_m(\gamma) P_o$ and the rate of $\log_2\left[1+\frac{L_S}{I_{PK}+\sigma_0^2}\right]$ (in b/s/Hz) where $I_{PK} = S_{PK}\left|\frac{1}{\sqrt{N}}\sum_{l=0}^{L-1} h_{FPSl} e^{-\frac{j2\pi lk*}{N}}\right|^2$ represents the interference from PU to SR with $S_{PK} = KS_P$, and

$h_{FPSl} = h_0 d_{PS}^{-\frac{\alpha}{2}} h_{Fl}$. Therefore, the SU link rate can be expressed as

$$C_{SU} = E\left\{[1 - P_f(\gamma)]P_v\log_2\left[1+\frac{L_S}{\sigma_0^2}\right]\right.$$

$$\left. + P_m(\gamma) P_o \log_2\left[1+\frac{L_S}{I_{PK}+\sigma_0^2}\right]\right\}\text{(in b/s/Hz).} \tag{12}$$

4. Objective function and optimal threshold

We aim at maximizing the weighted sum of the achieved PU and SU rates while guaranteeing the minimum PU rate, i.e., the optimization problem can be written as Maximize

$$f(\gamma) = \mu C_{PU} + (1-\mu)C_{SU}. \tag{13}$$

subject to

$$C_{PU} \geq \varphi\, C_{PUo}, \ 0 \leq \varphi \leq 1 \tag{14}$$

where $C_{PUo} = E\left\{\lambda\log_2\left[1+\frac{L_{PK}}{\sigma_0^2}\right]\right\}$ (in b/s/Hz) represents the achieved PU rate in the absence of SU, and $0 \leq \mu \leq 1$ is selected to emphasize the relative importance between the PU and the SU link rates. Substituting Equations (11) and (12) into (13), the objective function becomes $f(\gamma) = ae^{-\frac{\gamma}{\sigma_0^2+\sigma_x^2}} + be^{-\frac{\gamma}{\sigma_0^2}} + c$ where

$$a = \mu\frac{P_o}{K}E\left\{\log_2\left[1+\frac{L_{PK}}{\sigma_0^2}\right] - \log_2\left[1+\frac{L_{PK}}{I_S+\sigma_0^2}\right]\right\}$$

$$- (1-\mu)P_o E_i\left\{\log_2\left[1+\frac{L_S}{I_{PK}+\sigma_0^2}\right]\right\},$$

$$b = -(1-\mu)P_v E\left\{\log_2\left[1+\frac{L_S}{\sigma_0^2}\right]\right\}\leq 0,$$

$$c = \mu\left(\lambda - \frac{P_o}{K}\right)E\left\{\log_2\left[1+\frac{L_S}{\sigma_0^2}\right]\right\}$$

$$+ (1-\mu)\frac{P_o}{K}E\left\{\log_2\left[1+\frac{L_P}{I_S+\sigma_0^2}\right]\right\}$$

$$+ P_v E_{all}\left\{\log_2\left[1+\frac{L_S}{\sigma_0^2}\right]\right\}.$$

Taking the first derivative of Equation (13), $f'(\gamma) = \frac{-a}{(\sigma_0^2+\sigma_X^2)}e^{-\frac{\gamma}{\sigma_0^2+\sigma_X^2}} - \frac{b}{\sigma_0^2}e^{-\frac{\gamma}{\sigma_0^2}}$. and letting $f'(\gamma) = 0$, we get $\gamma = \frac{\sigma_0^2}{\sigma_x^2}(\sigma_0^2 + \sigma_x^2)\ln\left(-\frac{b}{a}\frac{\sigma_0^2+\sigma_x^2}{\sigma_0^2}\right)$.

The steady point is the maximum if it satisfies the following relation

$$f''(\gamma) = -\frac{a}{\left(\sigma_0^2 + \sigma_x^2\right)^2} e^{-\frac{\gamma}{\sigma_0^2 + \sigma_x^2}} + \frac{b}{\left(\sigma_0^2\right)^2} e^{-\frac{\gamma}{\sigma_0^2}} < 0.$$

Since b is non-positive, only a needs to be discussed. For $a > 0$ and $f''(\gamma) < 0$, the optimal threshold can be written as

$$\gamma^* = \max(0, \gamma), \gamma$$
$$= \frac{\sigma_0^2}{\sigma_X^2}\left(\sigma_0^2 + \sigma_X^2\right) \ln\left(-\frac{b}{a}\frac{\sigma_0^2 + \sigma_X^2}{\sigma_0^2}\right). \quad (15)$$

For $a \le 0$, $f(\gamma)$ would be maximum as $\gamma \to \infty$, corresponding to the case in which ST transmits without monitoring the PU transmission status.

Furthermore, the constraint (14) implies that $e^{\frac{-\gamma}{\sigma_x^2 + \sigma_0^2}} \ge \frac{\Delta C_{PK\varphi}}{\Delta C_{PK}}$, where $\Delta C_{PK\varphi} = \left[1 - \frac{K\lambda(1-\varphi)}{P_0}\right] E_i\left\{\log_2\left[1 + \frac{L_{PK}}{\sigma_0^2}\right]\right\} - E_i\left\{\log_2\left[1 + \frac{L_{PK}}{I_S + \sigma_0^2}\right]\right\}$ (in b/s/Hz) denotes the actual PU capacity loss and $\Delta C_{PK} = E_i\left\{\log_2\left[1 + \frac{L_{PK}}{\sigma_0^2}\right] - \log_2\left[1 + \frac{L_{PK}}{I_S + \sigma_0^2}\right]\right\}$ (in b/s/Hz) denotes the *target* PU capacity loss due to interference from the SU in K frequency slots. Since $e^{\frac{-\gamma}{\sigma_x^2 + \sigma_0^2}}$ and ΔC_{PK} are both non-negative, when $\Delta C_{PK\varphi} \le 0$, the constraint on the guaranteed target minimum PU rate is always satisfied, i.e., SU can use the optimal threshold derived in (15). Moreover, by solving the inequality above, the constraint on the threshold can be derived

$$\gamma \le \left(\sigma_0^2 + \sigma_x^2\right) \ln\left(\frac{\Delta C_{PK}}{\Delta C_{PK\varphi}}\right)$$

In summary, the capacity maximization optimal threshold which guarantees a certain PU link rate can be written as
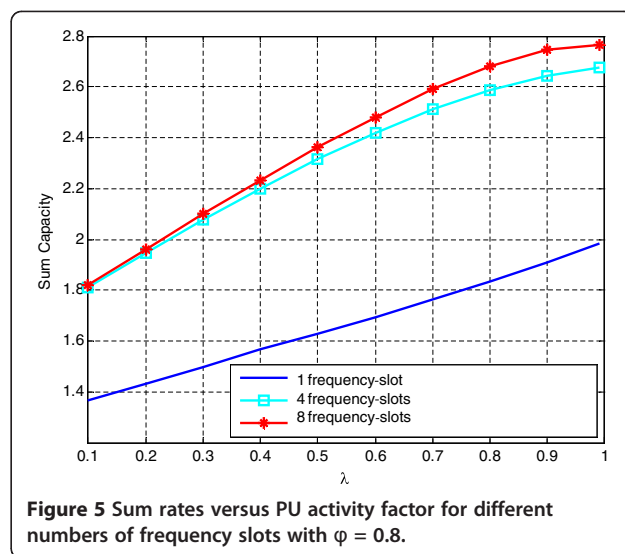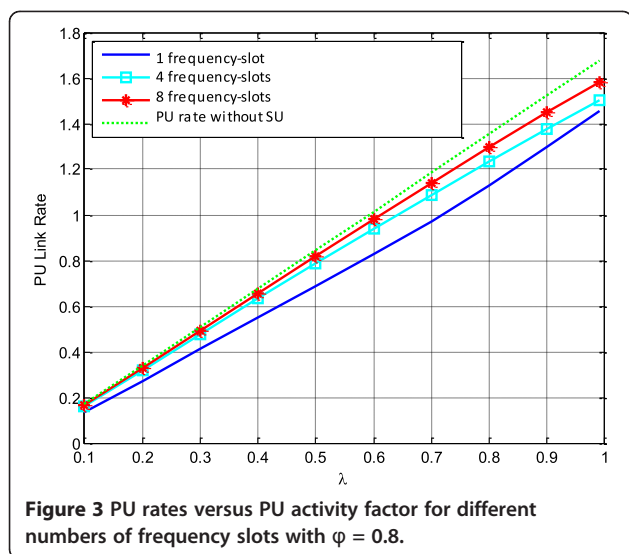
It is worth noting that, under the setting of $\varphi = 1$ (i.e., the guaranteed minimum PU rate is set exactly at its achievable rate in the absence of the SU), $\Delta C_{PK\varphi} = \Delta C_{PK}$, and $\gamma^{K\varphi} = 0$, indicating that the SU is never allowed to transmit.

5. Illustrative results
5.1. Simulation method
The network model in Figure 1 is used to set up the simulation. The locations of SU and PU's transmitters and receivers are generated in the same way as the full location case introduced in [4]. However, the channel realization is more complicated for the wideband channel model. At first, a $K \times 3000K$ binary matrix (allocation matrix) is generated for each radio location set of K subcarriers, and $3000K$ channel realizations. In each row of this matrix, the proportion of ones and zeros is equal to $\lambda/(1 - \lambda)$, but the positions of the ones and zeros are uniform randomly distributed from row to row. This binary matrix is used to represent the occupied/vacant situation of the licensed band.

For each radio location set, two $L \times 3000K$ matrices of samples of $h_{FPl} = h_0 \cdot d_P^{-\frac{\alpha}{2}} h_{Fl}$ and $h_{FPSl} = h_0 d_{PS*}^{-\frac{\alpha}{2}} h_{Fl}$ are generated first with $3000K$ realizations where L is the number of resolvable paths and is set to 4 in the simulation. The matrices of h_{FPl} and h_{FPSl} are processed by FFT to obtain samples of and $L_{PK} = S_{PK}\left|\frac{1}{\sqrt{N}}\sum_{l=0}^{L-1} h_{FPl} e^{-\frac{j2\pi lk^*}{N}}\right|^2$ $I_{PK} = S_{PK}\left|\frac{1}{\sqrt{N}}\sum_{l=0}^{L-1} h_{FPSl} e^{-\frac{j2\pi lk^*}{N}}\right|^2$, which are organized as two $K \times 3000K$ matrices. Two $K \times 3000$ matrices of L_S, I_s samples are also generated. After performing $E\{.\}$ and setting $\mu = 0.5$, a and b can be calculated to derive the optimal threshold. Another $K \times 3000K$ random matrix is generated in the same way as L_{PK}, I_{PK} but with the channel $H_k = S_{PK}\left|\frac{1}{\sqrt{N}}\sum_{l=0}^{L-1} h_{FPSl*} e^{-\frac{j2\pi lk}{N}}\right|^2$, where $h_{FPSl*} = h d_{PS*}^{-\frac{\alpha}{2}} h_{Fl}$ for each row. By dot-multiplying H_K by the allocation matrix then adding thermal noise, the detected signal sample matrix Y_K is obtained. Next, to calculate $P_f(\gamma)P_v$ and $P_m(\gamma)P_o$, two counters are used. For each column of Y_K, the minimum value is compared with the corresponding threshold γ. If it is larger than γ and corresponds to a

$$\gamma^{K\varphi} = \begin{cases} \infty \text{ if } a \le 0, & \text{and } \Delta C_{PK\varphi} \le 0 \\ \left(\sigma_0^2 + \sigma_X^2\right) \ln\left(\frac{\Delta C_{PK}}{\Delta C_{PK\varphi}}\right) \text{ if } a \le 0, & \text{and } \Delta C_{PK\varphi} > 0 \\ \left(\sigma_0^2 + \sigma_X^2\right) \min\left\{\max\left\{0, \frac{\sigma_0^2}{\sigma_X^2}\ln\left(-\frac{b}{a}\frac{\sigma_0^2 + \sigma_X^2}{\sigma_0^2}\right)\right\}, \ln\left(\frac{\Delta C_{PK}}{\Delta C_{PK\varphi}}\right)\right\} \text{ if } a > 0, & \text{and } \Delta C_{PK\varphi} > 0 \\ \left(\sigma_0^2 + \sigma_X^2\right) \max\left\{0, \frac{\sigma_0^2}{\sigma_X^2}\ln\left(-\frac{b}{a}\frac{\sigma_0^2 + \sigma_X^2}{\sigma_0^2}\right)\right\} \text{ if } a > 0, & \text{and } \Delta C_{PK\varphi} \le 0 \end{cases} \quad (16)$$

Figure 3 PU rates versus PU activity factor for different numbers of frequency slots with φ = 0.8.

Figure 5 Sum rates versus PU activity factor for different numbers of frequency slots with φ = 0.8.
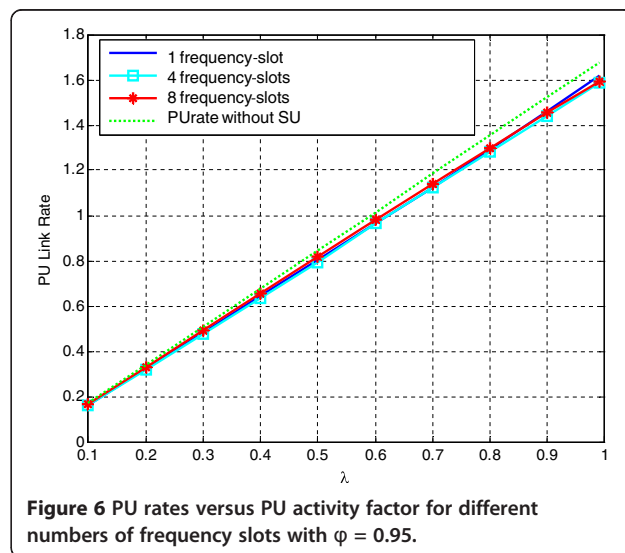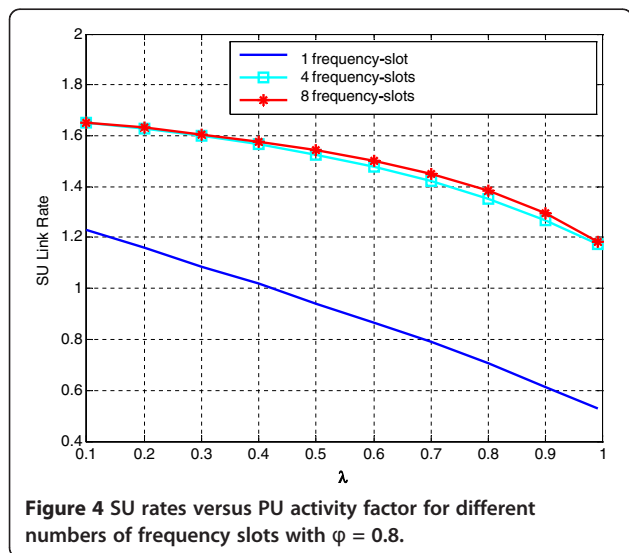
vacant frequency slot (i.e., element in the allocation matrix with value of 0), then the false alarm counter is increased by one. Similarly, if it is smaller than γ and the corresponding value in the allocation matrix is 1, then the miss detection counter is increased by one. Eventually by dividing the false alarm counts by the number of zeros experienced across each column, $P_f(\gamma)P_v$ is obtained. $P_m(\gamma)P_o$ is taken as the ratio of the miss detection counts to the number of 1's experienced across each column. For each radio location set, the same procedure is performed. Eventually, C_{PU}, C_{SU} are calculated according to Equations (11) and (12).
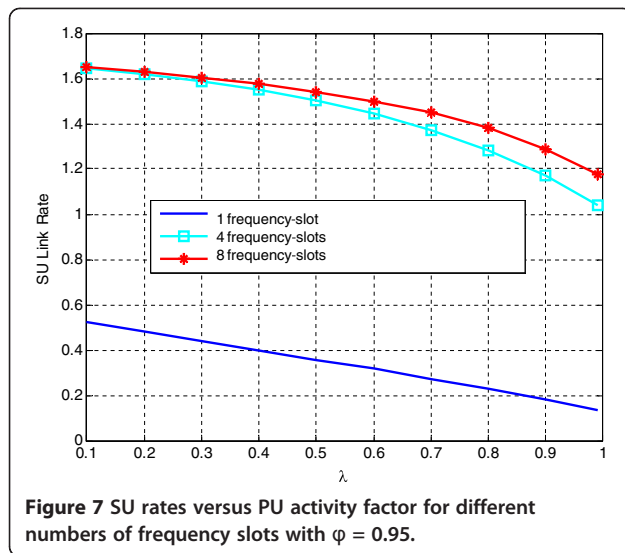
5.2. Results and discussion

Figures 3, 4, and 5 plot the PU, SU link rates, and sum rate (in b/s/Hz) versus the PU activity factor λ, respectively, for constraint of $0.8C_{PUo}$ where C_{PUo} is also included in Figure 3 for reference. While the PU link rate is within the

permitted range (as shown in Figure 3), the results plotted in Figure 4 indicate that the constraint on guaranteed minimum PU rate largely decreases the achievable SU link rate in the narrow-band case (i.e., one frequency slot), as compared to the wideband sensing scheme (i.e., four or eight frequency slots). As a result, the wideband sensing and spectrum access strategy maintain much higher SU link rate and eventually deliver a much more overall network capacity (sum rate) as shown in Figure 5.

Moreover, it is interesting to notice that it exhibits a trend that the more candidate subcarriers SU can choose from, the better SU link rate can be achieved. This is confirmed numerically for a stringent requirement of guaranteed PU minimum rate with φ = 0.95. The corresponding PU, SU, and sum rates (in b/s/Hz) versus the PU activity factor λ are plotted in Figures 6, 7, and 8, respectively. The best achievable PU rate C_{PUo} (in the

Figure 4 SU rates versus PU activity factor for different numbers of frequency slots with φ = 0.8.

Figure 6 PU rates versus PU activity factor for different numbers of frequency slots with φ = 0.95.

Figure 7 SU rates versus PU activity factor for different numbers of frequency slots with $\varphi = 0.95$.

absence of SU) is also plotted in Figure 6 for reference. Comparing the results in Figures 4 and 7 indicates that, when λ increases, the achieved SU rate is decreased to maintain the guaranteed PU minimum rate. Higher guaranteed PU minimum rate reduces the achieved SU rate. For the guaranteed PU rate increase of 15% (from $0.8C_{\mathrm{PU}o}$ in Figure 4 to $0.95C_{\mathrm{PU}o}$ in Figure 7), the achieved SU rate drops by more than 50% for narrowband sensing (i.e., single frequency slot), and less than 20% for wideband sensing (for four or eight frequency slots). The gain in the achieved SU rate due to wideband sensing is more pronounced at higher PU activity factor λ.

Since the objective of our optimization problem is to maximize the weighted sum rate while guaranteeing the minimum PU rate ($C_{\mathrm{PU}} \geq \varphi C_{\mathrm{PU}o}$, $0 \leq \varphi < 1$), it can be expected that the sum rate is non-decreasing with λ as
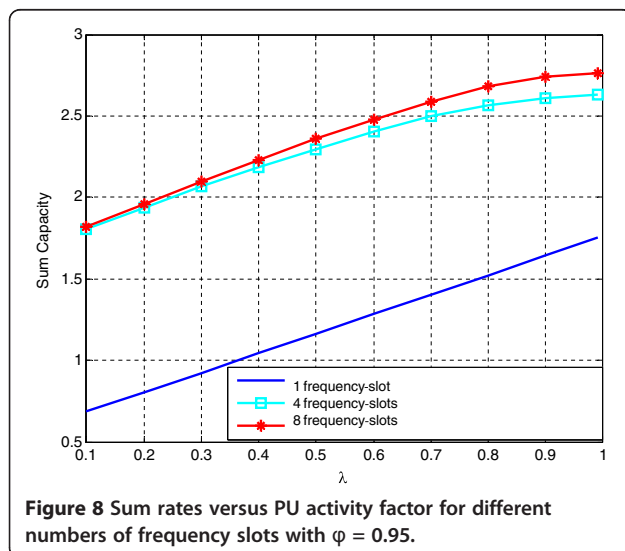
shown in Figures 5 and 8. However, at high value of λ (approaching 1), the achieved sum rate becomes saturated. This trend indicates that CR operation with SU sharing the PU spectrum band is more efficient at low PU activity.

6. Conclusion

In this article, the design of optimum sensing threshold for capacity maximization while guaranteeing the required minimum PU link rate is investigated for SU with wideband sensing capability. SU selects the *idle* frequency slot to access corresponding to the minimum measured PU beacon power exceeding the optimum sensing threshold. The wideband sensing capability along with the proposed access strategy helps the SU to reduce the miss detection probability and to increase its achievable link rate. Illustrative results show that, compared to the narrowband sensing, the wideband sensing approach offers a much better SU link rate and network sum capacity over the whole range of PU transmission activity factor and the resulting SU and sum rates increase monotonically with the number of sensed frequency slots while meeting stringent constraints on the guaranteed minimum PU rates.

Endnote

[a]Part of this article was presented at the IEEE VTC2011-Fall Conference in San Francisco, September 5–8, 2011.

References
1. S Haykin, Cognitive radio: brain-empowered wireless communications. IEEE. J. Sel. Areas Commun. **23**(2), 201–220 (2005)
2. FCC, Spectrum policy task force report ET Docket. Technical Report, 02–155 (2002)
3. FCC, *Federal communications commission spectrum policy task force FCC Report of the Spectrum Efficiency Working Group* (FCC, Technical Report 2002)
4. P Jia, M Vu, T Le-Ngoc, S Hong, V Tarokh, Capacity- and Bayesian-based cognitive sensing with location side information. IEEE. J. Sel. Areas Commun. **29**(2), 276–289 (2010)
5. N Maziar, A survey of cognitive radio access to tv/white spaces. Int. J. Digital Multimed. Broadcast **11** (2010). doi:10.1155/2010/236568. Article ID 236568

Figure 8 Sum rates versus PU activity factor for different numbers of frequency slots with $\varphi = 0.95$.